Research Article | Vol. 31, No. 19 / 11 Sep 2023 / Optics Express 30911
Optics EXPRESS

Optical heating-induced spectral tuning of supercontinuum generation in liquid core fibers using multiwall carbon nanotubes

YING WAN,[1,2,3] XUE QI,[2] JOHANNES HOFMANN,[2] RAMONA SCHEIBINGER,[2] GUOBIN JIA,[2] FENGJI GUI,[2] JONATHAN PLENTZ,[2] JIANXIANG WEN,[3] AND MARKUS A. SCHMIDT[2,4,5,*]

[1]*Jiangsu Key Laboratory for Optoelectronic Detection of Atmosphere and Ocean, Institute of Optics and Electronics, Nanjing University of Information Science & Technology, 219 Ningliu Road, Nanjing 210044, China*
[2]*Leibniz Institute of Photonic Technology, Albert-Einstein-Str. 9, 07745 Jena, Germany*
[3]*Key Lab of Specialty Fiber Optics and Optical Access Networks, Joint International Research Laboratory of Specialty Fiber Optics and Advanced Communication, School of Communication and Information Engineering, Shanghai University, 99 Shangda Road, Shanghai 200444, China*
[4]*Otto Schott Institute of Material Research, Friedrich Schiller University Jena, Fraunhoferstrasse 6, 07743 Jena, Germany*
[5]*Abbe Center of Photonics and Faculty of Physics, Friedrich-Schiller-University Jena, Max-Wien-Platz 1, 07743 Jena, Germany*
[*]*markus-alexander.schmidt@uni-jena.de*

Abstract: In this work, we demonstrate the optical heating modulation of soliton-based supercontinuum generation through the employment of multi-walled carbon nanotubes (MW-CNTs) acting as fast and efficient heat generators. By utilizing highly dispersion-sensitive liquid-core fibers in combination with MW-CNTs coated to the outer wall of the fiber, spectral tuning of dispersive waves with response times below one second via exploiting the strong thermo-optic response of the core liquid was achieved. Local illumination of the MW-CNTs coated fiber at selected points allowed modulation of the waveguide dispersion, thus controlling the soliton fission process. Experimentally, a spectral shift of the two dispersive waves towards the region of anomalous dispersion was observed at increasing temperatures. The presented tuning concept shows great potential in the context of nonlinear photonics, as complex and dynamically reconfigurable dispersion profiles can be generated by using structured light fields. This allows investigating nonlinear frequency conversion processes under unconventional conditions, and realizing nonlinear light sources that are reconfigurable quickly.

1. Introduction

Supercontinuum (SC) sources are in a wide range of applications such as nonlinear imaging [1], light switching [2], optical coherence metrology [3], and spectroscopy [4,5]. One successful effect employed is the soliton-based supercontinuum generation (SCG) [6], originating from the fission of higher-order solitons and the associated emission of dispersive waves (DWs). Recently, efficient SCG has been demonstrated in liquid-core fibers (LCFs), consisting of silica fiber-type capillaries filled with inorganic liquids [7–9], providing long light/matter interaction lengths and strong mode confinement (an overview about this field can be found in Ref. [10]). One remarkable feature of this type of fiber is the extension of the coherence limit [11], defined by the soliton number, beyond that of solid-glass fibers, which results from a non-instantaneous contribution to the nonlinear response function in case liquids are used. Since efficient SCG demands tailoring dispersion, various methods for dispersion control have been developed, e.g., nanofilms coated fiber [12], tapered fiber [13,14], and tailored photonic crystal fibers [15]. Due

#496199 https://doi.org/10.1364/OE.496199
Journal © 2023 Received 23 May 2023; revised 11 Aug 2023; accepted 13 Aug 2023; published 5 Sep 2023

Optics EXPRESS

to very high thermo-optic coefficients approaching those of semiconductors [16], dispersion of LCFs can be controlled via temperature [17,18], thus offering fast dispersion adjustments and reversibility. However, currently employed experimental realizations using Peltier elements [17] have slow response times and limitations regarding feasible temperature patterns, defining a clear demand for conceptually new approaches.

Carbon-based nanomaterials provide very efficient absorption of electromagnetic radiation and are therefore used for photothermal therapies [19,20], solar steam generation [21], as blackbody absorbers [22], and photoactuators [23]. Such photothermal materials enable the efficient generation of temperature profiles that are stable over long periods of time [22,24]. Multiwalled carbon nanotubes (MW-CNTs) have gained significant attention recently due to their unique optical and thermal properties. Specifically, they absorb across a wide range of wavelengths due to π-band optical transitions [20]. Additionally, they have an overall low specific heat capacity (0.50 – 0.75 J/kg/K)), thereby accelerating the heating and cooling process. Here, the integration of carbon-based materials with optical fibers is a promising area of research, as it offers the potential to incorporate optoelectronic functionality into fibers [25–27]. Combining carbon-based materials with optical fibers, therefore, presents a promising opportunity to control SCG through optical-induced temperature tuning. In this work, we introduce the concept of light-induced thermal tuning of SCG based on LCFs coated with MW-CNTs. Specifically, MW-CNT layers are deposited on the cladding of CS_2-filled LCFs and illuminated by external light, thus allowing to modulate the dispersion of a higher-order fiber mode with response times of the order of seconds or below. This optical heating-induced dispersion modulation scheme allows SC spectra to be tuned through changing the power of external modulating light, which, to our knowledge, is the first time this has been experimentally demonstrated.

2. Concept of light-induced thermal tuning of SCG

The concept of optical heating-induced tuning of SCG using MW-CNTs is shown in Fig. 1(a): The LCF considered in this work is composed of a fiber-type silica capillary filled with carbon disulfide (CS_2, core diameter: 3.65 µm, cladding diameter: 80.0 µm). As shown in various works [17,18], the dispersion and in particular the group-velocity dispersion (GVD) of higher-order modes (e.g., TE_{01} or TM_{01}) in such fibers strongly depend on the local temperature. This feature is unique to LCFs and results from the very large thermo-optical coefficients of inorganic liquids, which reach values similar to semiconductors [28]. Crucial for exploiting the temperature dependence in the context of soliton-based SCG is the strong dependence of DWs on waveguide dispersion due to the underlying phase-matching condition between soliton and DW [14,29]:

$$n(\lambda_s, T) + (\lambda_{DW} - \lambda_s)\frac{dn}{d\lambda}(\lambda_s) + \frac{\gamma P_s \lambda_{DW}}{4\pi} = n(\lambda_{DW}, T) \tag{1}$$

where n is the effective refractive index of the TE_{01} mode in CS_2-filled LCFs, which closely depends on the working wavelength (λ) and temperature (T). λ_{DW} and λ_s are the wavelengths of the DW and soliton, respectively. γ is the nonlinear parameter, which can be expressed by $\gamma = 2\pi n_2/(\lambda_s A_{eff})$ (with the effective mode field area A_{eff} of the LCF and the nonlinear refractive index n_2 of CS_2). P_s is the peak power of the assumed first soliton, given by $P_s = P_0(2N-1)^2/N^2$ (with input peak power P_0 and soliton number N [13,17]). According to Eq. (1), the wavelength at which DWs are formed is spectrally dependent on the temperature as schematically shown in Figs. 1(b) and 1(c): As temperature increases ($T_2 > T_1$, orange and green curves), the short- and long-wavelength DWs (DW1 and DW2) red- and blue-shift, respectively. In this way, the output SC spectra can be tuned via light-induced temperature changes in the CS_2-filled LCF.

To exploit this effect in the context of optical heating-induced tuning, the fiber is considered to be coated from outside with MW-CNT layers, acting as a strong light absorber to convert the power of externally applied light to heat, while having no impact on waveguide dispersion

Optics EXPRESS

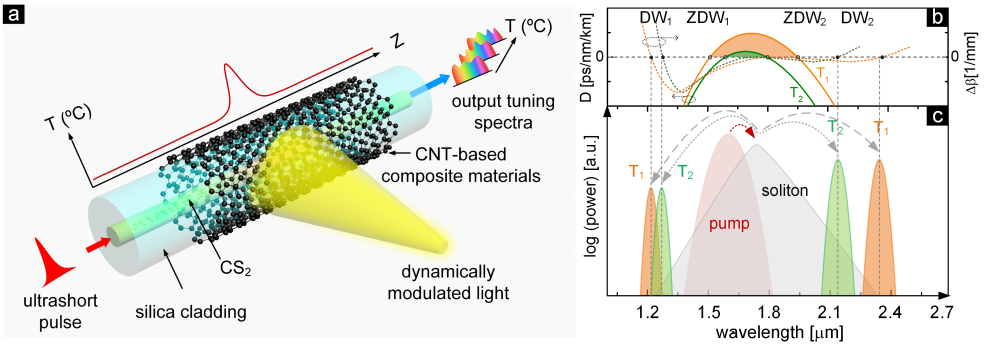

Fig. 1. (a) Illustration of the concept of light-induced thermal tuning of SCG based on CNT-based composite material coated onto the walls of CS_2-filled LCFs. (b) Example of spectral distribution of group velocity dispersion (D) and DW-phase-matching ($\Delta\beta$) in LCF at different temperatures. The orange and green curves refer to two DWs at two different temperatures ($T_1 < T_2$). (c) Illustration of the soliton-DW energy conversion process and the temperature-induced spectral shift of the DWs (gray: soliton, red: pump).

or modal attenuation. The temperature distribution inside the central liquid can thus be locally controlled by adjusting the irradiation position and light intensity of the external modulation laser source (MLS).

To reveal the impact of temperature on GVD, the GVD of the TE_{01} mode considering the above-discussed LCF is simulated by solving the dispersion equation of a step-index fiber [30]. The calculated result is illustrated in Fig. 2. Here, the material dispersions of CS_2 and silica are taken from Refs. [11,31] considering a temperature-dependent refractive index (RI) dispersion model for CS_2 [17] (see Eq. (2), where B_1 and C_1 are temperature dependent functions, with B_2 and C_2 being constants. The values of these parameters, including their temperature dependence, can be found in Table 1 of Ref. [17]):

$$n(\lambda, T) = (1 + \frac{B_1(T)\lambda^2}{\lambda^2 - C_1^2(T)} + \frac{B_2\lambda^2}{\lambda^2 - C_2^2})^{1/2} \tag{2}$$

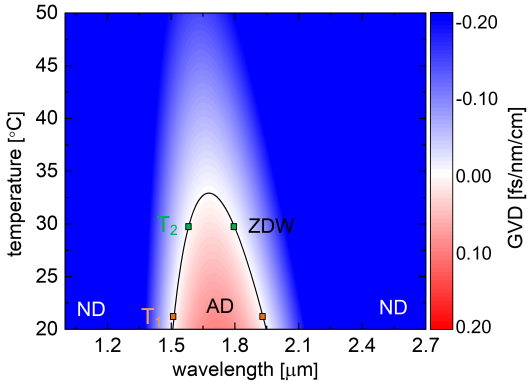

Fig. 2. Dispersion properties and temperature dependence of the relevant mode. (a) Calculated GVD of the TE_{01}-mode of the CS_2-filled LCF (core diameter: 3.65 μm) as a function of temperature and wavelength. The black line indicates the ZDWs, separating the domains of anomalous dispersion (AD, red) and normal dispersion (ND, blue). The actual values of the GVD are given by the color bar on the right.

Optics EXPRESS

The TE_{01} mode shows two zero dispersion wavelengths (ZDWs) encompassing an interval of anomalous dispersion (AD), as presented in Fig. 2. Note that the AD-interval is located in the vicinity of λ=1.55 μm which covers the bandwidth of ultrafast fiber laser used in the experiments. In case the temperature of the CS_2 core is increased, the ZDWs spectrally converge closer and closer to the temperature at which the AD range completely disappears and the dispersion is normal of all wavelengths considered.

3. Methods

The coating of MW-CNTs of the walls of the silica-based LCF involves the following steps: To prepare the coating solution, 92.75 wt% of PH 1000 (poly (3,4-ethylene dioxythiophene) polystyrene sulfonate (PEDOT: PSS) suspension from Heraeus Clevios) suspension was mixed with 7 wt% ethylene glycols (EG). 0.25 wt% Triton X-100 (Sigma Aldrich) was added to achieve better wettability to the surface of the silica cladding. Note that the PEDOT acts as polymer support holding together the CNTs. 20 mg of the functionalized MW-CNTs (MWCNTs-COOH from Ossila, the outer and inner diameter of 25 nm and 5-10 nm, length: 10-20 μm) was added to 0.5 ml of the prepared (PEDOT: PSS): EG: Triton x-100 mixture under strong stirring, forming the coating composite. The fiber considered was a 10-cm-long thin-diameter fiber-type capillary, having an inner and outer diameter of 3.58 μm and 79.43 μm, respectively. Note that for effective heat transfer, this fiber had a much smaller outer diameter than conventional fibers (typically 125 μm). This fiber was coated by brushing the composite, followed by subsequent drying at 60 °C for 10 min. By repeating this procedure, a black coating consisting of multiple layers of MW-CNTs of coated total thicknesses between 20 nm to 50 nm can be realized on the glass fibers. Figures 3(a)-(c) show a cross-section and a side view of the coated fiber, as well as a detailed image of the coating composite with MW-CNTs and PEDOT.

To uncover the optical properties of the composite, the spectral distributions of absorption, reflection, and transmission were studied on a reference borosilicate glass (borofloat, SCHOTT) substrate sample with a thickness of 1.1 mm and one coated with the MW-CNTs/PEDOT: PSS composite. Since the process for producing the MW-CNT coating on the substrate and the fiber outer surface is identical, nearly the same thickness of the carbon nanotubes (between 20 nm to 50 nm) is achieved. Experimentally, an Ulbricht sphere was employed to measure the transmission (T) and the reflection (R). Note that (R) includes the scattered light. The absorption (A) is calculated from the relation A=1-T-R (Fig. 3(d)). Particularly important is the very high absorption of the layer of more than 80% across the entire spectral domain ranging from 350 nm to 1500 nm (green curve). This is mainly due to its rough surface (Fig. 3(c)) and the absorption of the super-black material resulting from the optical transitions of its π-bands. At the long-wavelength side (>1500 nm), the reflection of the layer starts to increase and the absorption drops noticeably. The fluctuations observed in the absorption spectra (Fig. 3(d)) for wavelengths >850 nm stem from a transition to a different detector within the employed spectrometer.

Efficient filling of CS_2 through capillary action (c.f. Granzow et al. [32]; Washburn et al. [33]) and coupling of light were ensured by home-build optofluidic mounts (more details on the preparation procedure of LCFs can be found in our previous works [14,34]). The volatility of CS_2 is not of concern here, as the fluid is encapsulated in optofluidic holders that allow simultaneous optical and fluidic access (c.f. Fig. 8(d) of [10]), making the samples stable over a long time [32]. It is straightforward to verify that the core hole is filled with the solvent, as light will not propagate within the core if the core hole is not filled or contains a bubble. The experimental setup for optical heating-induced tuning of SCG (TE_{01} mode) consisted of an ultrafast fiber laser (Toptica FemtoFiber pro IR, central wavelength 1560 nm, repetition rate 80 MHz, pulse duration 36 fs), an s-waveplate, the MW-CNTs coated CS_2-filled LCF sample, a MLS, as well as in- and out-coupling lenses and diagnostics (for details see Fig. S1 of Supplement 1). Note that the function of the s-waveplate is to convert the linear polarized Gaussian input beam to a

Optics EXPRESS

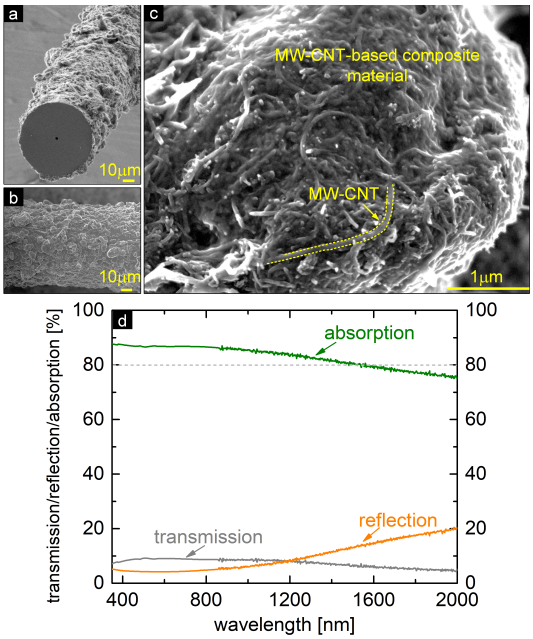

Fig. 3. Properties of the MW-CNT-based composite material coating located on the fiber surface. (a)-(c) Scanning-electron-micrograph (SEM) images of the coating material. (a) Cross-sectional and (b) side views. (c) Close-up-view of the composite coating material that primarily contains MW-CNTs and PEDOT. (d) Spectral distribution of transmission, reflection, and absorption of the composite material. Note that the contribution of light scattering is included in the reflection (see main text for details).

ring-shaped beam with azimuthal polarization in order to efficiently excite the TE_{01}-mode. A coupling efficiency of about 15.8% has been achieved, considering the fiber attenuation and the reflections at the various interfaces. Note that recent experiments have shown that the coupling efficiency can be improved by a factor of 3 by enlarging the hole diameter at the beginning of the fiber through post-processing (i.e., by using an uptaper). The input and output modes were imaged with a cooled InGaAs camera (ABS Jena IK1513) or a phosphorized CMOS camera (DataRay WinCamD-IR), while the azimuthal output polarization was checked by rotating a polarizer (LPNIRA050-MP2, Thorlabs, USA) inserted between the output lens and camera. Notice that under typical experimental conditions, such as those used in the present work, the generated spectra show a very high inter-spectra correlation, i.e. the associated noise is vanishingly small. This is consistent with our previous studies [14,34], which showed that SCG in CS_2-based liquid-core fibers exhibits a high degree of first-order coherence. To characterize the various spectral features, suitable bandpass filters were inserted into the beam path (pump: 1550±5 nm, short-wavelength DW: <1300 nm, long-wavelength DW: >2300 nm). The maximum output power of the pump laser (average power 160 mW) was used in all experiments, and no signs of degradation were observed at any time. The conditions of our experiments, including environmental temperature and light incoupling, remained constant far beyond the measurement period, as proven by additional long-term stability measurements. Moreover, in a previous work we have been able to demonstrate long-term stable SCG in liquid core fibers [35]. For spectral characterization, the output light was guided to a Fourier transform infrared (FTIR) spectroscope (OSA305, Thorlabs, USA) using an InF_3 patch cable (MF12L2, Thorlabs, USA).

Optics EXPRESS

To exploit the broadband absorption of the composite material as efficiently as, a broadband single-mode white light source (Superk compact, NKT photonics) covering large fractions of the visible and near-IR spectral domain (450 nm to 2400 nm) was selected as MLS. The output power and repetition rate of this pulsed MLS mounted sidewise to the LCF were fixed at 80 mW and 20000 Hz respectively. This repetition rate is so high that due to the long integration time of the FTIR spectrometer (several seconds), individual illumination pulses cannot be temporally resolved and many pulses from the illumination source contribute to one output spectrum. The highest possible repetition rate was chosen to heat the fiber as constantly as possible, overall yielding 81 mW of modulation light power across the entire emitted spectrum. It should be noted that, as shown in simulations (details in Supplement 1, Fig. S3) the LCF system is so inert from a thermal point of view that the pulsed laser radiation can be considered like continuous wave (CW) radiation. As the area of the light beam (diameter: 3 mm) is substantially larger than that of the fiber, only a fraction of the power of the modulation light (3.4%) is actually absorbed by the MW-CNTs. Here, the reason for not using a focusing lens is that no modulation of the supercontinuum is visible for smaller illumination lengths. To adjust the modulation light power, a tunable attenuator (NDL-25S-2, Thorlabs, USA) was placed between the sample and MLS.

To reveal the dynamics of the dispersion tuning, an in-house made real-time power measurement system (Fig. S2) was implemented. This system allows to simultaneously measure the changes in modulated power of MLS and SC spectrum using an oscilloscope (TDS5104, Tektronix, USA), power meter (PM, Thorlabs, USA), and a photodetector (PD, PDA10DT-EC, Thorlabs, USA).

4. Experimental results and discussion

The first step in the experimental characterization refers to the measurement of the spectral modification of the SC when the MW-CNTs coated LCF is illuminated with different MLS powers and at different positions (relative to the fiber input) (Fig. 4). Here, the black curve represents the output SC spectra in case no external light is applied, i.e., at room temperature. Two distinct DWs appear on both sides of the AD domain, located within the bands 1170 nm $<\lambda<$ 1350 nm and 2100 nm $<\lambda<$ 2550 nm, respectively (highlighted by the purple areas in Fig. 4).

Each colored curve in Fig. 4(a) refers to an output spectrum at a different level of power of the MLS in case the point of heating was z=2 cm. When the power of the MLS increases, the wavelengths at which the short- and long-DWs have their maximum shift towards the AD domain, i.e., the domain of the pump laser. This effect can be explained by the fact that with increasing modulation power of the MLS, a local change of the temperature distribution in the fiber core (here RI reduction due to the negative thermo-optical coefficient of CS_2) is imposed, which influences modal dispersion and thus the soliton fission process (i.e., wavelength of the DWs). Similar spectral changes were observed for electrically heated fibers [17], indicating that light-induced temperature control of MW-CNTs coated LCFs provides an alternative method for temperature tuning of SCG. When the modulation point is 5 cm (z=5 cm) away from the fiber input, the long- and short-wavelength DWs show the same trend. However, the red-shift is not obvious for the short-wavelength DW while the long-wavelength DW blue-shifts more strongly than in the z=2 cm case, hence leading to the flatter spectrum in the IR region. This is probably because the location of the modulation light beam (z=5 cm) is far away from the location of soliton fission happening (z=2 cm) where the first pair of DWs generated. At z=5 cm, the decrease of dispersion around the soliton wavelength induced by the increased MLS powers provides more chances and smoothens the output spectrum. The spectral smoothening is caused by the newly happened soliton fission process induced by the local temperature change. In Fig. 4(a) and (b), there is a slight difference in the unmodulated supercontinuum spectra (P=0 mW), which is mainly due to the slight shift of the coupling position in LCF caused by the environmental vibration. However, no fluctuations of the supercontinuum output are visible when the samples are illuminated. Note that the mode profiles in the spectral intervals of the

Optics EXPRESS

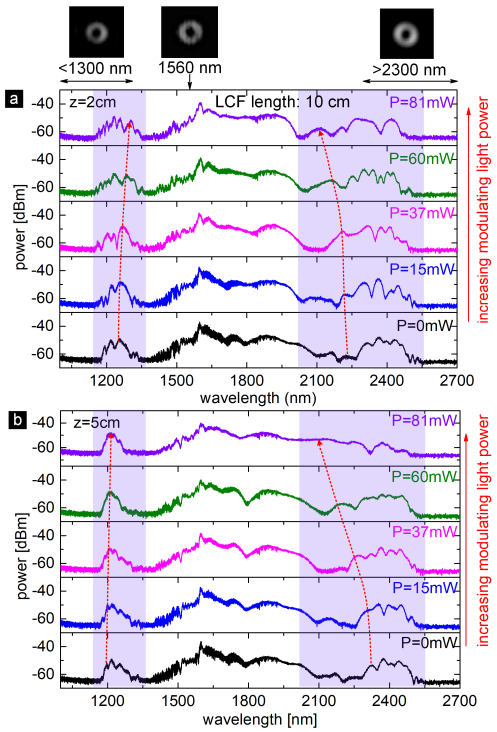

Fig. 4. Experimental demonstration of optical heating-induced spectral tuning of SCG in MW-CNTs coated LCF. The plots show the spectral distribution of the nonlinear frequency conversion process in at the output when increasing the power of the MLS at two different positions of the external light exposure ((a) z=2 cm, (b) z=5 cm, see also Fig. S1). The black curve represents the output spectrum without external irradiation (MLS is off). The numbers on the top right of each plot refer to the emitted average power of the MLS. The red dashed lines with arrows are guide-to-the-eyes indicating the DW tuning with increasing modulation light power. The purple areas refer to the spectral domains in which the spectral variation is mostly visible. The top images show measured mode profiles within three different wavelength intervals when the MLS is turned on.

pump and both DWs show the characteristic dough-nut shape of a TE_{01} mode and do not change during the experiment.

After confirming that temperature-induced wavelength shifts can be generated via MW-CNT-mediated light absorption, the dynamics of the heating and cooling processes were determined using the setup mentioned in the Method sections (Fig. S2). This result is depicted in Fig. 5. Comparing the SC spectra without and with MLS (z=2 cm, P=37 mW), as designated by the navy and red curves in Fig. 5(a), their spectra show clear differences in the spectral range from 2170 nm to 2300 nm, as the corresponding spectral density is significantly increased when the MLS is switched on. In addition, some peaks with small changes are observed at 2300-2400 nm from the soliton fission before the temperature-modulated part in the beginning part of the LCF. This spectral range at 2300-2400 nm can thus be used as an indicator to reveal the system's dynamics and was experimentally selected (navy and red shading) by using a bandpass filter (Laser Components GmbH, LO147745, center wavelength: 2211 nm, bandwidth: 82 nm). The corresponding power dynamics of MLS and LCF output were measured for different modulation frequencies. In this way, the response times of absorption-induced heating and cooling processes of the MW-CNTs coated LCF were determined. Overall, the power of the LCF output (green

Optics EXPRESS

curve) follows the behavior of the MLS (blue curve) with a delay in the range of seconds. To quantify the corresponding time constants, the cooling and heating processes were evaluated separately (Fig. 5(c), corresponding to red dashed regions in Fig. 5(b)). Here, the signal rise and decay times, corresponding to heating and cooling are about 0.47 s and 1.01 s, respectively, matching the order-or-magnitude observed in simulations (Fig. S3). Note that the heating-related response time is twice as long as that of the cooling process, which can be explained by the limited interaction area between the modulating light and the MW-CNTs. As during heating the fiber is illuminated only from one side, thus half of the MW-CNTs material remains unexposed. During cooling, however, heat can dissipate along all directions, so cooling is faster than heating. Compared with the electrical Peltier element-based heating [17,18], the light-induced heating method has a much shorter response time (on the order of seconds), which is mainly due to the much lower heat capacity of the MW-CNT layer compared with the Peltier elements used in the electrical modulation scheme (response time several minutes).

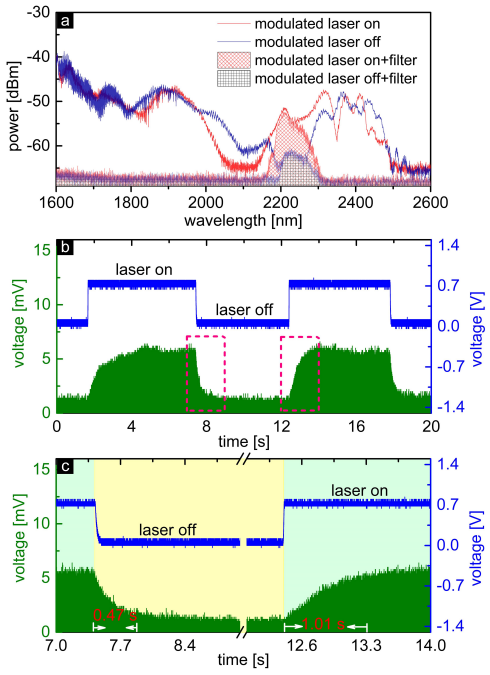

Fig. 5. Response time measurement of optical heating-induced tuning of SCG. (a) SC spectra generated in MW-CNTs coated LCF with and without modulation light exposure. The curves that include hatched areas refer to the spectra after using a bandpass filter (center wavelength: 2211 nm, bandwidth: 82 nm). (b) Temporal measurements of the change of the output power after the filters, in case the modulation light is periodically switched on and off. The green curve represents the power of the filtered output detected by the fast photo diode, while the blue curve refers to the output power of the modulation light. (c) Close-up of the two areas highlighted by the red dashed rectangles in (b), showing the time domains of heating and cooling.

5. Summary and outlook

In this work, optical heating modulation of soliton-based SCG through the employment of MW-CNTs acting as fast and efficient heat generators is demonstrated. Highly dispersion-sensitive LCFs in combination with MW-CNTs coated to the outer wall of the fiber allow for spectral

Optics EXPRESS

tuning of DWs with response times below one second via exploiting the strong thermo-optic response of the core liquid (CS_2). Via local illumination of the MW-CNTs coated fiber at selected points along the fiber, modulation of the dispersion of the waveguide and thus modification of the soliton fission process was achieved. A spectral shift of the two DWs towards the region of AD was observed in the experiment at increasing temperatures. The presented tuning concept includes great potential in the context of nonlinear photonics, as complex and dynamically reconfigurable dispersion profiles can be generated by using light fields that are structured in intensity distribution. This allows investigating the nonlinear frequency conversion process under unconventional conditions, and realizing of nonlinear light sources that are reconfigurable quickly and thus be optimized via artificial intelligence.

Future research may aim to accelerate the modulation even further by directly heating the core region through the use of heat-absorbing species such as plasmonic nanoparticles, highly absorbing dyes, or quantum dots. Additionally, the use of LCFs with lower heat capacity (e.g., with smaller outer diameter) can additionally speed up heat absorption and dissipation.

Funding. China Scholarship Council (202106890056); Deutsche Forschungsgemeinschaft (JU 3230/1-1, QI 140/2-1, SCHM 2655/11-1, SCHM 2655/12-1, SCHM 2655/3-2); Startup Foundation for Introducing Talent of Nanjing University of Information Science and Technology (2023r090); Natural Science Research of Jiangsu Higher Education Institutions of China (23KJB140014).

Acknowledgments. The authors thank Barbara Geisenhainer (Leibniz-IPHT) for the transmission, reflection, and absorption measurements, and Dr. Jan Dellith (Leibniz-IPHT) for the SEM measurements. The authors also acknowledge support by the German Research Foundation Projekt-Nr. 512648189 and the Open Access Publication Fund of the Thueringer Universitaets- und Landesbibliothek Jena.

Disclosures. The authors declare no conflict of interests.

Author Contribution. Ying Wan: Conceptualization (equal); Data curation (lead); Formal analysis (equal); Investigation (lead); Methodology (lead); Resources (equal); Visualization (lead); Writing – original draft (equal). Xue Qi: Formal analysis (equal); Investigation (equal); Resources (supporting); Writing – review & editing (equal). Johannes Hofmann: Investigation (equal); Investigation (supporting); Resources (supporting); Writing – review & editing (equal). Ramona Scheibinger: Formal analysis (equal); Investigation (supporting); Resources (supporting); Writing – review & editing (equal). Fengji Gui: Methodology (supporting); Writing – review & editing (supporting). Guobin Jia: Conceptualization (equal); Data curation (equal); Formal analysis (supporting); Resources (equal); Writing – review & editing (supporting). Jonathan Plentz: Data curation (supporting); Formal analysis (supporting); Resources (supporting); Writing – review & editing (supporting). Jianxiang Wen: Formal analysis (supporting); Investigation (supporting); Resources (supporting); Funding acquisition (equal). Markus A. Schmidt: Conceptualization (lead); Formal analysis (equal); Funding acquisition (lead); Project administration (lead); Supervision (lead); Writing – review & editing (lead).

Data availability. The data that support the findings of this study are available from the corresponding author upon reasonable request.

Supplemental document. See Supplement 1 for supporting content.

References

1. A. Rampur, D.-M. Spangenberg, B. Sierro, P. Hänzi, M. Klimczak, and A. M. Heidt, "Perspective on the next generation of ultra-low noise fiber supercontinuum sources and their emerging applications in spectroscopy, imaging, and ultrafast photonics," Appl. Phys. Lett. **118**(24), 240504 (2021).
2. O. Melchert, C. Brée, A. Tajalli, A. Pape, R. Arkhipov, S. Willms, I. Babushkin, D. Skryabin, G. Steinmeyer, U. Morgner, and A. Demircan, "All-optical supercontinuum switching," Commun. Phys. **3**(1), 146 (2020).
3. T. Udem, R. Holzwarth, and T. W. Hänsch, "Optical frequency metrology," Nature **416**(6877), 233–237 (2002).
4. M. K. Dasa, C. Markos, M. Maria, C. R. Petersen, P. M. Moselund, and O. Bang, "High-pulse energy supercontinuum laser for high-resolution spectroscopic photoacoustic imaging of lipids in the 1650-1850 nm region," Biomed. Opt. Express **9**(4), 1762–1770 (2018).
5. M. Halloran, N. Traina, J. Choi, T. Lee, and J. Yoo, "Simultaneous measurements of light hydrocarbons using supercontinuum laser absorption spectroscopy," Energy Fuels **34**(3), 3671–3678 (2020).
6. N. Singh, M. Xin, D. Vermeulen, K. Shtyrkova, N. Li, P. T. Callahan, E. S. Magden, A. Ruocco, N. Fahrenkopf, C. Baiocco, P. B. Kuo, S. Radic, E. Ippen, F. X. Kartner, and M. R. Watts, "Octave-spanning coherent supercontinuum generation in silicon on insulator from 1.06 μm to beyond 2.4 μm," Light: Sci. Appl. **7**(1), 17131 (2018).
7. S. Junaid, W. Huang, R. Scheibinger, K. Schaarschmidt, H. Schneidewind, P. Paradis, M. Bernier, R. Vallée, S.-E. Stanca, G. Zieger, and M. A. Schmidt, "Attenuation coefficients of selected organic and inorganic solvents in the mid-infrared spectral domain," Opt. Mater. Express **12**(4), 1754–1763 (2022).

Optics EXPRESS

8. D. Michalik, T. Stefaniuk, and R. Buczyński, "Dispersion management in hybrid optical fibers," J. Lightwave Technol. **38**(6), 1427–1434 (2019).
9. C. Wang, G. Feng, W. Li, J. Men, X. Chen, C. Yang, and S. Zhou, "Effect of temperature on supercontinuum generation in CS_2-core optical fiber," IEEE Photonics J. **10**(5), 1–11 (2018).
10. M. Chemnitz, S. Junaid, and M. A. Schmidt, "Liquid-core optical fibers-a dynamic platform for nonlinear photonics," Laser Photonics Rev. **11**, 2300126 (2023).
11. M. Chemnitz, M. Gebhardt, C. Gaida, F. Stutzki, J. Kobelke, J. Limpert, A. Tünnermann, and M. A. Schmidt, "Hybrid soliton dynamics in liquid-core fibres," Nat. Commun. **8**(1), 42 (2017).
12. T. A. Lühder, M. Chemnitz, H. Schneidewind, E. P. Schartner, H. Ebendorff-Heidepriem, and M. A. Schmidt, "Tailored multi-color dispersive wave formation in quasi-phase-matched exposed core fibers," Adv. Sci. **9**(8), 2103864 (2022).
13. T. Birks, W. Wadsworth, and P. S. J. Russell, "Supercontinuum generation in tapered fibers," Opt. Lett. **25**(19), 1415–1417 (2000).
14. X. Qi, R. Scheibinger, J. Nold, S. Junaid, M. Chemnitz, and M. A. Schmidt, "Axial dispersion-managed liquid-core fibers: A platform for tailored higher-order mode supercontinuum generation," APL Photonics **7**(11), 116106 (2022).
15. S. Junaid, J. Bierlich, A. Hartung, T. Meyer, M. Chemnitz, and M. A. Schmidt, "Supercontinuum generation in a carbon disulfide core microstructured optical fiber," Opt. Express **29**(13), 19891–19902 (2021).
16. M. J. Weber, *Handbook of Optical Materials* (Chemical Rubber Company, 2018).
17. M. Chemnitz, R. Scheibinger, C. Gaida, M. Gebhardt, F. Stutzki, S. Pumpe, J. Kobelke, A. Tünnermann, J. Limpert, and M. A. Schmidt, "Thermodynamic control of soliton dynamics in liquid-core fibers," Optica **5**(6), 695–703 (2018).
18. R. Scheibinger, J. Hofmann, K. Schaarschmidt, M. Chemnitz, and M. A. Schmidt, "Temperature-sensitive dual dispersive wave generation of higher-order modes in liquid-core fibers," Laser Photonics Rev. **17**(1), 2100598 (2023).
19. S. Ghosh, S. Dutta, E. Gomes, D. Carroll, R. D'Agostino Jr, J. Olson, M. Guthold, and W. H. Gmeiner, "Increased heating efficiency and selective thermal ablation of malignant tissue with DNA-encased multiwalled carbon nanotubes," ACS Nano **3**(9), 2667–2673 (2009).
20. L. M. Maestro, P. Haro-González, B. Del Rosal, J. Ramiro, A. Caamano, E. Carrasco, A. Juarranz, F. Sanz-Rodríguez, J. G. Solé, and D. Jaque, "Heating efficiency of multi-walled carbon nanotubes in the first and second biological windows," Nanoscale **5**(17), 7882–7889 (2013).
21. Y. Wang, L. Zhang, and P. Wang, "Self-floating carbon nanotube membrane on macroporous silica substrate for highly efficient solar-driven interfacial water evaporation," ACS Sustainable Chem. Eng. **4**(3), 1223–1230 (2016).
22. Y. Ito, Y. Tanabe, J. Han, T. Fujita, K. Tanigaki, and M. Chen, "Multifunctional porous graphene for high-efficiency steam generation by heat localization," Adv. Mater. **27**(29), 4302–4307 (2015).
23. K. Czaniková, N. Torras, J. Esteve, I. Krupa, P. Kasák, E. Pavlova, D. Račko, I. Chodák, and M. Omastová, "Nanocomposite photoactuators based on an ethylene vinyl acetate copolymer filled with carbon nanotubes," Sens. Actuators, B **186**, 701–710 (2013).
24. J. U. Kim, S. Lee, S. J. Kang, and T. Kim, "Materials and design of nanostructured broadband light absorbers for advanced light-to-heat conversion," Nanoscale **10**(46), 21555–21574 (2018).
25. Y. Zuo, W. Yu, C. Liu, X. Cheng, R. Qiao, J. Liang, X. Zhou, J. Wang, M. Wu, Y. Zhao, P. Gao, S. Wu, Z. Sun, K. Liu, X. Bai, and Z. Liu, "Optical fibres with embedded two-dimensional materials for ultrahigh nonlinearity," Nat. Nanotechnol. **15**(12), 987–991 (2020).
26. J. Chen, Y. Xiong, F. Xu, and Y. Lu, "Silica optical fiber integrated with two-dimensional materials: towards opto-electro-mechanical technology," Light: Sci. Appl. **10**(1), 78 (2021).
27. G. Jia, J. Plentz, J. Dellith, A. Dellith, R. A. Wahyuono, and G. Andrä, "Large area graphene deposition on hydrophobic surfaces, flexible textiles, glass fibers and 3d structures," Coatings **9**(3), 183 (2019).
28. S. Pumpe, M. Chemnitz, J. Kobelke, and M. A. Schmidt, "Monolithic optofluidic mode coupler for broadband thermo-and piezo-optical characterization of liquids," Opt. Express **25**(19), 22932–22946 (2017).
29. J. M. Dudley, G. Genty, and S. Coen, "Supercontinuum generation in photonic crystal fiber," Rev. Mod. Phys. **78**(4), 1135–1184 (2006).
30. A. W. Snyder and J. D. Love, *Optical Waveguide Theory*, vol. 175 (Chapman and Hall London, 1983).
31. J. W. Fleming, "Dispersion in GeO_2-SiO_2 glasses," Appl. Opt. **23**(24), 4486–4493 (1984).
32. N. Granzow, P. Uebel, M. A. Schmidt, A. S. Tverjanovich, L. Wondraczek, and P. S. J. Russell, "Bandgap guidance in hybrid chalcogenide–silica photonic crystal fibers," Opt. Lett. **36**(13), 2432–2434 (2011).
33. E. W. Washburn, "The dynamics of capillary flow," Phys. Rev. **17**(3), 273–283 (1921).
34. R. Scheibinger, N. M. Lüpken, M. Chemnitz, K. Schaarschmidt, J. Kobelke, C. Fallnich, and M. A. Schmidt, "Higher-order mode supercontinuum generation in dispersion-engineered liquid-core fibers," Sci. Rep. **11**(1), 5270 (2021).
35. K. Schaarschmidt, H. Xuan, J. Kobelke, M. Chemnitz, I. Hartl, and M. A. Schmidt, "Long-term stable supercontinuum generation and watt-level transmission in liquid-core optical fibers," Opt. Lett. **44**(9), 2236–2239 (2019).